

# Application of plasmonic subwavelength structuring to enhance infrared detection

David W. Peters,\* Paul S. Davids, Jin K. Kim, Darin Leonhardt, Thomas E. Beechem III, Stephen W. Howell, Taisuke Ohta, Joel R. Wendt, John A. Montoya  
Sandia National Laboratories, P.O. Box 5800, Albuquerque, NM, USA 87185-1082

## ABSTRACT

Nanoantennas are an enabling technology for visible to terahertz components and may be used with a variety of detector materials. We have integrated subwavelength patterned metal nanoantennas with various detector materials for infrared detection: midwave infrared indium gallium arsenide antimonide detectors, longwave infrared graphene detectors, and shortwave infrared germanium detectors.

Nanoantennas offer a means to make infrared detectors much thinner, thus lowering the dark current and improving performance. The nanoantenna converts incoming plane waves to more tightly bound and concentrated surface waves. The active material only needs to extend as far as these bound fields. In the case of graphene detectors, which are only one or two atomic layers thick, such field concentration is a necessity for usable device performance, as single pass absorption is insufficient. The nanoantenna is thus the enabling component of these thin devices. However nanoantenna integration and fabrication vary considerably across these platforms as do the considerations taken into account during design.

Here we discuss the motivation for these devices and show examples for the three material systems. Characterization results are included for the midwave infrared detector.

**Keywords:** nanoantenna, infrared, detector, metasurface, metamaterial

## 1. INTRODUCTION

Nanoantennas offer a method to improve infrared detector performance using existing infrared detector materials and through careful design, can usher in new infrared detector materials that are not currently feasible detector materials. In past efforts, we and others have designed [1-2] and fabricated [3] detectors using metallic top surfaces. Our effort is an extension of our prior design, fabrication, and characterization of perfect absorbers [4].

The concentration of the electromagnetic fields into small volumes is the fundamental advantage that the nanoantenna-based detectors offer over their traditional counterparts. This concentration allows the active layer to be a thin layer directly below the patterned nanoantenna layer. This thin layer could be a thinner layer of a traditional detector material such as HgCdTe or InAsSb. Thinner layers of these materials should lead to lower dark currents as the volume is lessened. It also allows greater freedom in utilizing strain to tailor the cutoff wavelength. The active layer could also be a more exotic material such as bilayer graphene (BLG), which would not be a viable detector material without a nanoantenna to concentrate the light.

Concentration of the fields occurs because the nanoantenna converts incoming plane waves into bound surface waves whose extent is limited to a small fraction of a free-space wavelength. When correctly designed, this conversion can have near 100% efficiency with no loss to reflection at the surface [4]. Moreover, unlike with thin films the reflection null does not change with angle of incidence and does not appreciably increase for incident angles approaching grazing incidence. The angle invariance is true for both polarizations. This angular acceptance cone is more than sufficient for detector applications.

The nanoantenna pattern may be varied from pixel to pixel on a focal plane array allowing for different pixels to have different functionalities. This could include changes in the center wavelength or bandwidth for multispectral imaging. Polarized designs would allow for snapshot polarimetry.

\* dwpeter@sandia.gov

Our nanoantenna designs vary depending on the bandwidth and fabrication constraints for a particular application. For the devices described in this paper, all use the square loop design that is common in many microwave frequency selective surface (FSS) applications.

## 2. GERMANIUM AND BILAYER GRAPHENE INFRARED DETECTORS

We have used nanoantennas on a variety of different detector platforms. Here we briefly describe two of these using germanium and bilayer graphene.

### 2.1 Germanium SWIR Detector

A nanoantenna-enabled germanium detector for the shortwave infrared (SWIR) can be made using a very thin layer of germanium. This should allow very fast operation. The ground plane for our device is an aluminum/copper alloy deposited on a silicon wafer. Polycrystalline germanium was evaporated directly onto this metal layer. E-beam lithography and a liftoff process were used to define the nanoantenna on the front surface. The detector was designed for a center absorption wavelength of 1.5μm as shown in the RCWA simulation of Fig. 1.

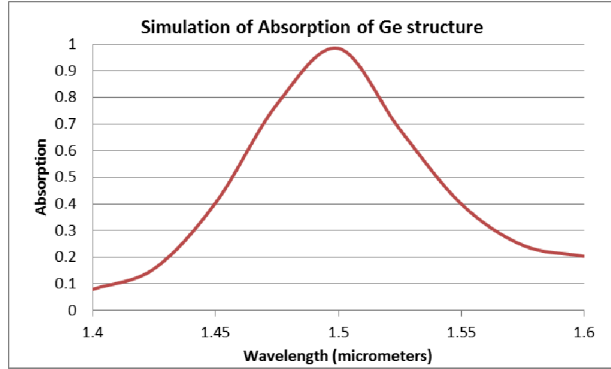


Fig. 1. Absorption of the nanoantenna-enabled germanium detector.

This design has been fabricated as seen in Fig. 2. We are awaiting characterization results.

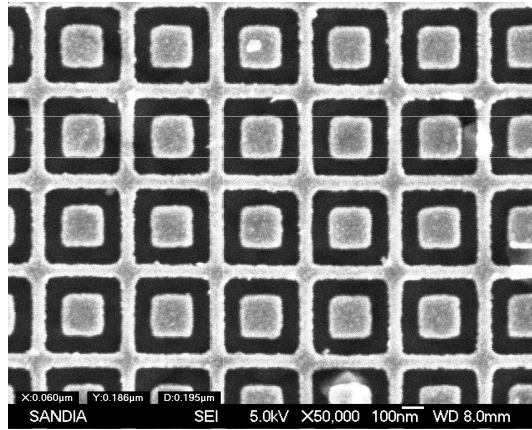


Fig. 2. Micrograph of patterned gold on a germanium detector. Gold pattern formed with e-beam and a liftoff process.

### 2.2 Bilayer Graphene LWIR Detector

Bilayer graphene (BLG), molybdenum disulfide, and other 2D materials have been considered for infrared detectors due to their mobility of carriers, inherent thinness, and a unique band structure that allows for very broadband detection via the creation of a bandgap commensurate with these wavelengths [5]. While the thinness of the material is one of its desirable qualities, it is also a liability when making a detector. The absorption of a plane wave through the two atomic

layers that comprise BLG is only 4.6%. Clearly this value is unacceptable even if 100% of those absorbed photons could be converted into measured charge carriers.

It is for this type of application that the nanoantenna does not merely improve performance, but makes a new device type possible. The tailoring of the electromagnetic fields through design of the patterned metal layer allows concentration of the field in the graphene layer. This can be seen in Fig. 3 where the field is concentrated in the BLG layer under one patterned metal surface and adjacent to the patterned metal used as a BLG contact. Fabrication of these devices to test the ability to tailor the electromagnetic field location to maximize absorption in the BLG is on-going.

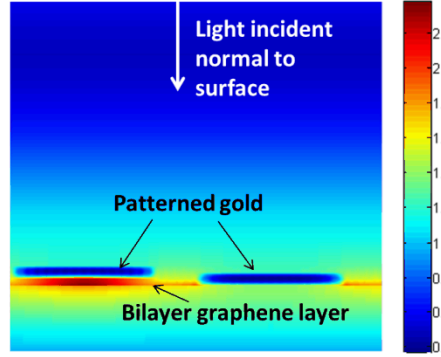


Fig. 3. RCWA simulation showing the magnetic field strength in arbitrary units for a wavelength of  $10.9\mu\text{m}$ . Strong fields are generated near a layer of bilayer graphene, which acts as a detector material.

### 3. DESIGN AND SIMULATION FOR INDIUM ARSENIDE ANTIMONIDE DETECTOR

Detectors using InAsSb already exist, however the incorporation of a nanoantenna offers opportunities for performance improvement. The fabrication process for these devices involves removal of the sacrificial GaSb wafer on which the epitaxial active layer is grown. Through this process we are left with the epitaxial layers sandwiched between the metal ground plane and the patterned layers of the nanoantenna. The steps in achieving this flipping, bonding, and subsequent substrate removal through etching requires additional epitaxial layers that are sacrificed in the fabrication process [1].

The remaining layers of the epitaxial stack are all accounted for in RCWA simulations. Nanoantenna parameters were varied to create three designs with resonance peaks in the MWIR. These three designs are shown in Fig. 4.

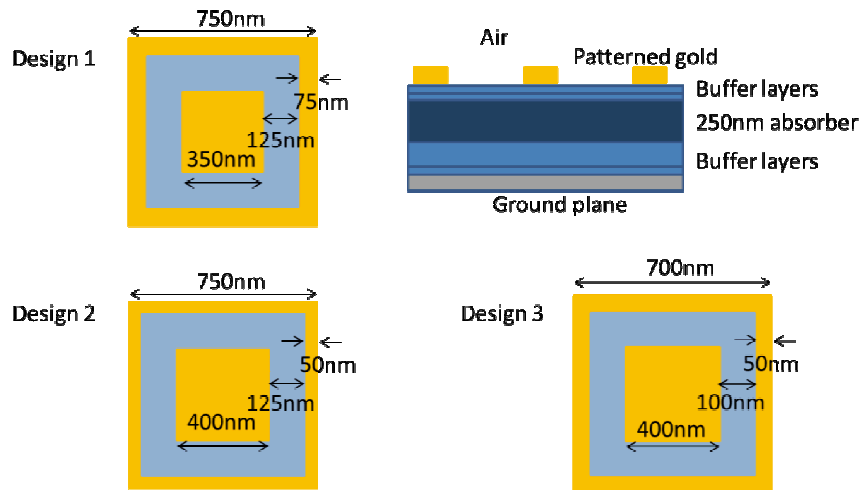


Fig. 4. Three designs for InAsSb detectors. All three designs, plus a no-nanoantenna control, were fabricated on the stack shown at upper right.

Results of the RCWA simulations of the three designs from Fig. 4 are shown in Fig. 5. The primary absorption peaks in the range of  $3.25\mu\text{m}$  to  $3.5\mu\text{m}$  have near unity absorption. The Design 2 and Design 3 absorption spectra are very similar in the wavelength range close to the primary resonance. However we can see differences in secondary resonances at shorter wavelengths. This demonstrates that the nanoantenna design space does not have a singular solution for a given desired resonance, even with a fixed design (in this case the square loop) and fixed spacing.

Clearly, an even larger design space is encountered if other frequency selective surface designs are considered. Also note that reflectionless designs can be found: this is similar to the results of the perfect absorber work of [4] in that we can make a broad angularly-insensitive nanoantenna with no reflection without the need to apply an antireflection coating.

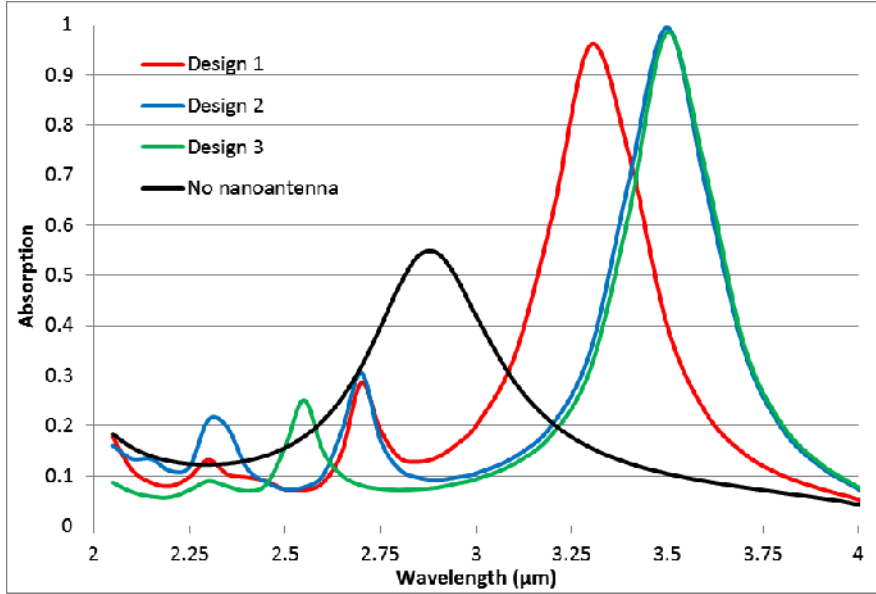


Fig. 5. Rigorous Coupled Wave Analysis (RCWA) simulation of total absorption in all layers for the InAsSb detector designs at normal incidence.

The three designs above were not optimized to maximize the absorption of the light in solely the active layer, but rather total absorption in the structure (minimized reflection from the top surface). Thus we are inadvertently including unwanted absorption in the metal layers and in the epitaxial layers outside the active layer. This further optimization step could result in even greater detector performance. In these designs approximately 40-50% of the absorbed light is absorbed in the active region. Since fabrication of these designs, optimized designs have shown that this value may be doubled.

#### 4. FABRICATION AND EXPERIMENTAL RESULTS

##### 4.1 Fabrication

The three designs for the MWIR detector of Fig. 4 were fabricated. The active and sacrificial layers of the detector are grown epitaxially on a GaSb substrate. To obtain the metal/semiconductor/metal sandwich required for the nanoantenna design, the epitaxial layers must be grown and then removed from their substrate. The growth stack on the GaSb substrate includes an InAsSb etch stop layer, a p-type GaSb contact layer, an  $\text{AlGa}_{0.15}\text{AsSb}$  electron barrier, a 250nm InAsSb absorber, and an  $\text{AlGa}_{0.15}\text{AsSb}$  absorber passivation layer.

A dry etch is then performed to define an electrical contact within the active region of the photodetector. Contact metal is deposited onto the p-type GaSb contact layer and onto the InAsSb absorber layer. The contact metal on the p-type GaSb layer also serves as the nanoantenna's electromagnetic ground plane. An indium bump is then deposited onto these electrical contacts. The wafer is diced for the hybridization of each test chip to a silicon fanout. The silicon fanout

is capable of reading individual nanoantenna pixels for their accurate characterization. The GaSb substrate and the InAsSb etch stop layer are then completely removed with the aid of mechanical polishing and selective chemical etching.

Once the substrate is removed, the backside is patterned with a nanoantenna pattern with the aid of e-beam lithography. The metallic patterns are composed of a thin 50nm Au layer to reduce electromagnetic loss in the metal and provide a strong resonance. The writing of this sample used ZEP520A electron beam resist developed in n-amyl acetate, exposed at 4nA with a step of 10nm on a JEOL JBX-9300FS e-beam lithography system.

#### 4.2 Characterization

Multiple photodetector pixels with the three nanoantenna designs and the control no-nanoantenna pixel were fabricated and packaged into a DIP for dark and photocurrent measurements in a cryostat. Then, the spectra response of these photodetectors (with and without integrated nanoantenna) was taken at 120K using a Nicolet 6700 Fourier transform infrared spectrometer.

The spectral quantum efficiency of the various photodetectors are normalized to a common peak value of 0.5 for their primary resonance peak and plotted in the figure for comparison of spectral shapes. The relative magnitudes do not have a meaning in this plot. Design 2 (Q2 in Fig. 6) and Design 3 (Q3 in Fig. 6) each have multiple pixels represented by curves in the plot.

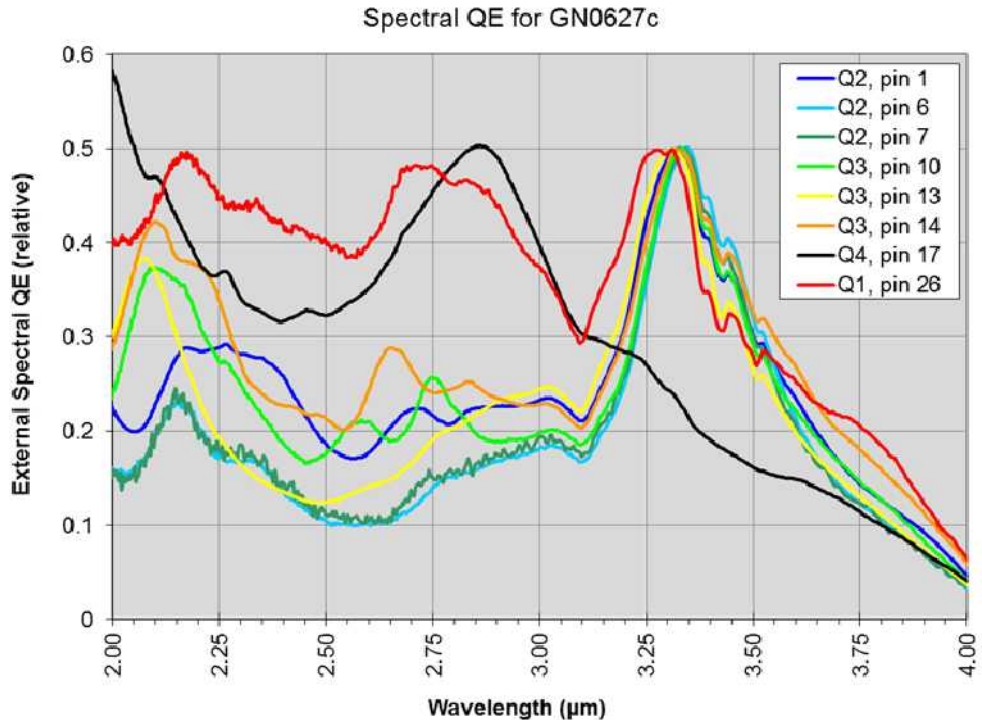


Fig. 6. Spectral quantum efficiency for III-V MWIR detector sample. QE's are individually scaled to a maximum of 0.5. (Q1 is Design 1; Q2 is Design 2; Q3 is Design 3; and Q4 is the control sample with no nanoantenna).

The measured resonances of the three nanoantenna samples and the control sample align relatively well with the simulation results. Additional measurements will be made to allow normalization of the vertical axis to determine the actual quantum efficiency.

## 5. CONCLUSIONS

Nanoantenna-enabled infrared detectors offer several advantages to traditional infrared detectors. The versatility of the nanoantenna concept is demonstrated here by the use of three different detector materials in three different wavelength bands inside the infrared: germanium for SWIR, bilayer graphene for LWIR, and InAsSb for MWIR.

The nanoantenna converts plane waves to concentrated surface waves that allow compact active layers. For the case of the graphene detector, the nanoantenna is a necessary component for achieving acceptable detector sensitivity by concentrating the incoming electric field into the plane of the graphene layer.

Fabrication processes have been developed for all of these devices, as it is not necessarily the standard detector fabrication process that is required. For the case of the InAsSb detectors we have shown preliminary results. These results confirm the results from the simulations, adding confidence to the design process.

## ACKNOWLEDGEMENT

Sandia National Laboratories is a multi-program laboratory managed and operated by Sandia Corporation, a wholly owned subsidiary of Lockheed Martin Corporation, for the U.S. Department of Energy's National Nuclear Security Administration under contract DE-AC04-94AL85000.

## REFERENCES

- [1] D. W. Peters, C. M. Reinke, P. S. Davids, J. F. Klem, D. Leonhardt, J. R. Wendt, J. K. Kim, S. Samora, "Nanoantenna-Enabled Midwave Infrared Focal Plane Arrays," *Infrared Technology and Applications XXXVIII*, edited by B. F. Andresen, G. F. Fulop, P. R. Norton, *Proc. of SPIE*, vol. 8353, 83533B, 2012.
- [2] S. Choi and K. Sarabandi, "Bowtie nanoantenna integrated with indium gallium arsenide antimonide for uncooled infrared detector with enhanced sensitivity," *Appl. Opt.*, vol. 35, pp. 8432-8438, Dec. 2013.
- [3] S. J. Lee, Z. Ku, A. Barve, J. Montoya, W.-Y. Jang, S. R. J. Brueck, M. Sundaram, A. Reisinger, S. Krishna, S. K. Noh, "A monolithically integrated plasmonic infrared quantum dot camera," *Nature Comm.*, vol. 2, 19 Apr. 2011.
- [4] D.W. Peters, P. Davids, J.R. Wendt, A.A. Cruz-Cabrera, S.A. Kemme, S. Samora, "Metamaterial-inspired high-absorption surfaces for thermal infrared applications," *Proc. of SPIE*, vol. 7609, 2010.
- [5] T.J. Echtermeyer, L. Britnell, P.K. Jasnos, A. Lombardo, R.V. Gorbachev, A.N. Grigorenko, A.K. Geim, A.C. Ferrari, K.S. Novoselov, "Strong plasmonic enhancement of photovoltage in graphene," *Nature Comm.*, vol. 2, 30 Aug. 2011.